

# TIME VARIANT POWER CONTROL IN CELLULAR NETWORKS

*Michael Andersin* \* and *Zvi Rosberg* †

(August 1996)

---

## Abstract

We study the transmission power control in a cellular network where users mobility results in a time varying gain matrix. A framework for evaluating the channel quality is specified, and an asymptotic representation of the link gain evolution in time is obtained. Then, a variant of a standard Distributed Constrained Power Control (DCPC) which copes with user mobility is derived. These two power controls, as well as constant-received power and constant-transmitted power controls are compared with respect to their outage probabilities in a Manhattan-like microcellular system. The comparison reveals that the classical DCPC algorithm has an outage probability close to one, unless some counter-measures are taken. The time variant algorithm however, copes well with users mobility and provides a close to an optimal scale up factor for the Signal to Interference Ratio (SIR) target. Furthermore, the time variant algorithm provides a substantial reduction in outage probability compared to the other algorithms above.

**Keywords:** PCS, Wireless, Power Control, Time Variant Gain Matrix, Mobility.

---

\*Telia Mobile, SE-131 86 Nacka Strand, Stockholm, Sweden.

†Haifa Research Lab., Science and Technology, MATAM, 31905 Haifa, Israel.

---

# 1 Introduction

Transmitter power control has proven to be an efficient method to control cochannel interference in cellular PCS, and to increase bandwidth utilization. Power control can also improve channel quality, lower the power consumption, and facilitate network management functions such as mobile disconnection, hand-offs, base-station selection and admission control.

Power control algorithms can be sub-divided into two main classes. One is the *constant-received-power* control, where transmitters adapt their power to meet some *received power target* at the receiver. The other is the *quality-based* power control, where the transmitters adapt their power to meet some *signal quality target* at the receiver. Quality-based power control has been shown to outperform constant-received-power control [32], and it has been extensively studied for narrow-band and wide-band systems.

Centralized and distributed algorithms with *continuous power levels, non-random interferers, and Signal to Interference (SIR) quality measure*, have been developed and their convergence properties have been investigated in [1, 2, 8, 12, 13, 14, 15, 18, 22, 23, 25, 32, 33]. Distributed algorithms with *continuous power levels, random interferers, and Signal to Interference (SIR) objectives*, have been studied in [24, 27]. Distributed power control with *discrete power levels and SIR quality measure*, has been studied in [4, 31], and with *continuous power control and Bit Error Rate (BER) quality measure*, in [20]. Resource management functions combined with power control have been also investigated. A combination with *mobile admission* has been studied in [5, 9]; a combination with *base station selection* in [19, 29]; and a combination with *mobile disconnection and hand-off* in [4]. Notably is the study in [30], where sufficient conditions have been derived for the convergence of power control algorithms, which unifies most of the known converging results.

In all the studies above, it has been assumed that the **power control converges much faster compared to the changes in the link gains due to mobility**. This assumption has motivated a snapshot evaluation of the algorithms (where link gains are fixed in time), which implies an under estimation of the quality measure target. (see e.g., [6]). To compensate this under estimation, coarse over-allocation of bandwidth is being used for designing

a cellular network. In future PCS environments, bandwidth would be more carefully allocated and users mobility will have a greater impact on the system performance. Hence, the snapshot analysis will not provide the desired system design parameters, and users mobility should be taken into account.

A preliminary study of time variant power control in [6], reveals that the quality measure target must be set significantly higher than the target which is determined under the snapshot assumption. The study however, does not provide any concrete rule to determine the actually required quality target. Determining this value is a primary engineering problem in power control and it is the main objective of the current paper. The authors are not aware of any previous results on this design problem.

This paper studies the “slow” power control problem in a cellular network where link gains vary in time according to a slow fading process which is exponentially correlated in time, [17]. An asymptotic representation of the link gain evolution in time is derived, and a framework to evaluate the channel quality in a time varying system is specified. In spite of the dynamic problem complexity, we derive a simple distributed time-dependent power control algorithm which successfully copes with users mobility. The algorithm enhances a previously proposed Distributed Constrained Power Control (DCPC) algorithm, [15], and requires only three additional system parameters. One is the maximum velocity of a mobile, the second is the log normal variance of the shadow fading, and the third is the correlation distance of the shadow fading. These three parameters can be a priori estimated by the system operator, therefore resulting in an algorithm that can be applied in practice.

Our numerical examples reveal that the DCPC algorithm has an outage probability close to one, unless some counter-measures are taken. One possible counter-measure is to bound the transmission power from below. Another, is to scale up the quality measure target. In the latter case, it is not clear however, with how much to scale up. The time dependent algorithm which we develop, copes with this situation and provides a close to an optimal scale up factor. The algorithm also provides a substantial improvement in the spectrum utilization compared to the DCPC algorithm enhanced with a lower bound on the transmission power, the constant-transmitted power algorithm, and the constant-received power algorithm.

In Section 2 we present the time variant system model, and in Section 3 we derive the power control algorithm. Numerical results are evaluated in Section 4, and final conclusions

are given in Section 5.

---

## 2 System Model

Consider a generic channel in a cellular network which is being accessed by  $N$  transmitters, where each one of them is communicating with exactly one receiver. For the uplink case, the transmitters are the mobiles and the receivers are their corresponding base stations. For the downlink case, their roles are reversed.

When transmitter  $j$  ( $1 \leq j \leq N$ ) is transmitting at time  $t$ , it uses a power of  $p_j(t) \leq \bar{p}_j$ , where  $\bar{p}_j$  is the maximum transmission power for transmitter  $j$ . Given that at time  $t$ , the link gain between transmitter  $j$  and receiver  $i$  is  $g_{ij}(t)$  ( $1 \leq i, j \leq N$ ), the received signal power at receiver  $i$  is  $g_{ii}(t) p_i(t)$ . The interference power experienced by receiver  $i$  at time  $t$ , is  $\nu_i + \sum_{j:j \neq i} g_{ij}(t) p_j(t)$ , ( $1 \leq i \leq N$ ), where  $\nu_i > 0$  is a time independent background noise power.

Define the Signal to Interference Ratio at receiver  $i$  at time  $t$ ,  $SIR_i(t)$ , by

$$SIR_i(t) = \frac{g_{ii}(t) p_i(t)}{\nu_i + \sum_{j:j \neq i} g_{ij}(t) p_j(t)}, \quad (1 \leq i \leq N). \quad (1)$$

The SIR is a standard measure for channel quality, which is highly correlated with its error rate. Let  $\gamma_i$  be the SIR target for the channel between transmitter  $i$  and its corresponding receiver. We say that channel  $i$  is *supported at time  $t$* , if

$$SIR_i(t) \geq \gamma_i. \quad (2)$$

To incorporate mobility of the transmitters or the receivers (uplink or downlink), which results in time variant link gains, we have to specify the link gain processes ( $g_{ij}(t) \mid t \geq 0$ ), ( $1 \leq i, j \leq N$ ).

We focus on a relatively slow power control algorithms with 1-100 power updates per second. Such rates are too slow to track fast multipath fading (usually modeled by a fast time varying Rayleigh process). Hence, we assume that the multipath fading is resolved by

appropriate coding and interleaving techniques. Power control algorithms with update rates of 100-10000 updates per second (which includes multipath fading) has been studied in [26].

For every time instant  $t$ , the link gain is modeled as a product of a distance dependent propagation loss, and a slow shadow fading component. That is,

$$g_{ij}(t) = L_{ij}(t) \cdot S_{ij}(t) . \quad (3)$$

*i* The factor  $L_{ij}(t)$  is modeled as,

$$L_{ij}(t) = D_{ij}^{-\alpha}(t) , \quad (4)$$

where  $D_{ij}(t)$  is the distance between transmitter  $j$  and receiver  $i$  at time  $t$ , and  $\alpha$  is a propagation constant. The factor  $S_{ij}(t)$  is assumed to be log-normally distributed with a log-mean of 0 dB, and a log-variance of  $\sigma^2$  dB. That is,

$$Z_{ij}(t) \stackrel{\text{def}}{=} \frac{10}{\sigma} \log_{10} S_{ij}(t) ,$$

is the standard normal random variable.

We assume that the link gain processes are mutually independent, and the evolution of each process ( $g_{ij}(t) \mid t \geq 0$ ) is governed by the following correlated process.

Let  $v$  be the average mobile velocity, and  $t_0$  be an arbitrary time reference. For every  $t > 0$ , we assume that ( $Z_{ij}(t) \mid t \geq 0$ ) is a stationary Gaussian process with an exponential correlation function given by,

$$E[Z_{ij}(t_0 + t)Z_{ij}(t_0)] = e^{-\frac{vt}{X}} , \quad (5)$$

where  $X$  is the effective correlation distance of the shadow fading. The parameter  $X$  is environment dependent and describes how rapid the fading correlation is decreasing as a function of distance.

From (5), we can represent the evolution of ( $Z_{ij}(t) \mid t \geq 0$ ) by

$$Z_{ij}(t_0 + t) = Z_{ij}(t_0) \cdot e^{-\frac{vt}{X}} + N_{ij}(t) \cdot \left(1 - e^{-\frac{2vt}{X}}\right)^{\frac{1}{2}} , \quad (6)$$

where  $\{N_{ij}(t)\}$  are independent standard normal random variables.

Observe that for every pair  $(i, j)$ , process.  $S_{ij}(t)$ ,  $t \geq 0$ , are identically distributed random variables. The time variant shadow fading process with the exponential correlation function in (5), has been proposed in [17] based on field experimental data.

For notational convenience, we introduce the *normalized velocity*,

$$u = \frac{2v}{X}. \quad (7)$$

The evolution in (6) then becomes,

$$Z_{ij}(t_0 + t) = Z_{ij}(t_0) \cdot e^{-\frac{ut}{2}} + N_{ij}(t) \cdot \left(1 - e^{-ut}\right)^{\frac{1}{2}}. \quad (8)$$

Assuming that the mobile moves with a constant velocity  $v$ , we can use the power expansion of the functions  $x^{-\alpha}$ ,  $e^{-x}$  and  $10^x$ , to obtain

$$L_{ij}(t_0 + t) = L_{ij}(t_0) + o(ut), \quad (9)$$

and

$$S_{ij}(t_0 + t) = S_{ij}(t_0) \left(1 + c \cdot (ut)^{1/2} \cdot N_{ij}(t)\right) \cdot 10^{o((vt)^{1/2})}, \quad (10)$$

where  $c = \frac{\sigma}{10} \ln(10)$ , and  $o(x)$  is a function of  $x$  with the property  $\lim_{x \rightarrow \infty} o(x)/x = 0$ .

To facilitate the derivation of a time variant power control, we use the following asymptotic representation with respect to  $(ut)^{1/2}$  (the standard deviation scale). For notational clarity, we adopt the convention of  $a \approx b$  to denote an equality  $a = b + o(x^{1/2})$  or  $a = b \cdot c^{o(x^{1/2})}$ .

From (3)-(10), it follows that

$$g_{ij}(t_0 + t) \approx g_{ij}(t_0) (1 + c \cdot (ut)^{1/2} \cdot N_{ij}(t)). \quad (11)$$

**Remark 2.1** Note that  $c \cdot (ut)^{1/2} \cdot N_{ij}(t)$  is normally distributed with mean 0 and standard deviation  $c \cdot (ut)^{1/2}$ . Thus, the link gain means within a short time interval are practically the same.

### 3 Time Variant Power Control

In this section, we propose a time variant version of the Distributed Constrained Power Control (DCPC) from [15]. We start by showing the limitation of the DCPC in a time variant system.

When the link gains vary in time, DCPC updates the power according

$$p_i(t + dt) = \begin{cases} \min \left\{ \bar{p}_i, \frac{\gamma_i}{g_{ii}(t)} \left( \nu_i + \sum_{j:j \neq i} g_{ij}(t) p_j(t) \right) \right\}, & \text{if } i \in U(t), \\ p_i(t), & \text{otherwise,} \end{cases} \quad (12)$$

where  $U(t)$  is an arbitrary set of transmitters. Observe that any asynchronous power update is allowed (subject to some weak conditions which exclude infinitely long intervals where a power is not being updated). If  $U(t) = \{1, \dots, N\}$  for every update instance  $t$ , then we get the synchronous DCPC algorithm. Otherwise, we get an arbitrary asynchronous version (ADCPC).

Also note, that the right element in the right-hand-side of the power iteration is the SIR target times the ratio between the interference power (including the background noise) at receiver  $i$ , and the link gain  $g_{ii}(t)$ . Since the interference power can be measured, and  $g_{ii}(t)$  can be detected by the transmitter from the base station pilot signal (assuming a reciprocal system), this algorithm can be implemented in a distributed manner.

In this paper, we consider a SIR based power control algorithm. An alternative approach is to use a Bit Error Rate (BER) based algorithm. Although BER is more directly connected to the user perceived quality than SIR is, it has the following deficiency. In practical systems bit errors are rare events. This makes BER estimators highly inaccurate, especially within the short time intervals that are imposed by fast power control updates.

In practice, the interference and the link gain of the allocated channel  $i$ , are evaluated by sampling and averaging. Thus, the implemented DCPC is actually

$$p_i(t + dt) = \begin{cases} \min \left\{ \bar{p}_i, \frac{\gamma_i}{\bar{g}_{ii}(t)} \left( \nu_i + \sum_{j:j \neq i} \bar{g}_{ij}(t) p_j(t) \right) \right\}, & \text{if } i \in U(t), \\ p_i(t), & \text{otherwise,} \end{cases} \quad (13)$$

where  $\{\bar{g}_{ij}(t)\}$  are averages of the link gains in a small time interval around  $t$ .

Under the assumption that link gains are fixed in time (i.e.,  $g_{ij}(t) = g_{ij}$ ), it has been shown in [15], that the iterated powers in (12) converge from every initial set of powers, to the following unique and positive fixed-point solution  $(p_1, p_2, \dots, p_N)$  of

$$p_i = \min \left\{ \bar{p}_i, \frac{\gamma_i}{g_{ii}} \left( \nu_i + \sum_{j:j \neq i} g_{ij} p_j \right) \right\}, \quad (1 \leq i \leq N). \quad (14)$$

When all the channels can be supported, this power vector is the minimum power vector (component-wise) which supports them at every time instant  $t$ . That is,  $SIR_i(t) = \gamma_i$  for every  $i$  and  $t$ .

However, in a cellular network mobiles change their positions, resulting in random and non-stationary link gains. To demonstrate the DCPC limitation in such an environment, consider the SIR values under the converging power vector in a slightly more favorable case where *the link gain means are stationary in time*. Assume that the sample averages have a highly statistically significant level so that the  $\{\bar{g}_{ij}(t)\}$  averages in (13) are practically the same as the theoretical stationary means (to be denoted by  $\{\bar{g}_{ij}\}$ ). In such a case, the iterated powers converge to the unique and positive fixed-point solution of

$$p_i = \min \left\{ \bar{p}_i, \frac{\gamma_i}{\bar{g}_{ii}} \left( \nu_i + \sum_{j:j \neq i} \bar{g}_{ij} p_j \right) \right\}, \quad (1 \leq i \leq N). \quad (15)$$

Observe however, that even in this case the equality in (15) involves only the mean link gains. Since the actual link gains are distributed around the means, the probability that each  $SIR_i(t)$  is below the SIR target could be too high. Therefore, it is very likely that none of the mobiles are supported. This indeed turned out to hold true in our numerical results.

To address this limitation we consider a more general case where the link gain means are not necessarily stationary, but the approximation in (11) holds true for every time reference  $t_0$  and small  $t$ . Fix an arbitrary time reference  $t_0$  (where the power vector is  $(p_1(t_0), \dots, p_N(t_0))$ ), and examine the iterated powers in (13) for  $t > t_0$ , given the link gain matrix realization at time  $t_0$ . (In probability theory terminology, we examine the iterated powers given the sub- $\sigma$ -field at time  $t_0$ .)

From (11),  $g_{ij}(t_0 + t)$  is random with respect to any realization instance  $g_{ij}(t_0)$ , and its variance increases linearly with  $t$ . Thus, up to some threshold  $t^*$ , the samples of the



interference and the link gain of the allocated channel may produce highly statistically significant estimates of the means. Therefore, given the link gain matrix at time  $t_0$ , we may from Remark 2.1, practically use the following equalities:

$$\bar{g}_{ij}(t_0 + t) \approx g_{ij}(t_0) , \quad (0 \leq t \leq t^*) . \quad (16)$$

Assume an ideal condition where the iterated power vector always converges within a time interval of length  $t^*$ , under some convergence stopping rule. (The time horizon  $t^*$ , will serve as a tuning parameter in our time-variant power control algorithm.) Under these conditions, it follows from (13), (15) and (16) that  $(p_1(t_0 + t^*), p_2(t_0 + t^*), \dots, p_N(t_0 + t^*))$  is a fixed-point solution of

$$p_i(t_0 + t^*) \approx \min \left\{ \bar{p}_i, \frac{\gamma_i}{g_{ii}(t_0)} \left( \nu_i + \sum_{j:j \neq i} g_{ij}(t_0) p_j(t_0 + t^*) t^* \right) \right\} , \quad (1 \leq i \leq N) , \quad (17)$$

for every realization of a gain matrix and a power vector at time  $t_0$ .

Consider a channel  $i$ , where the approximated equality in (17) is obtained by

$$p_i(t_0 + t^*) \approx \frac{\gamma_i}{g_{ii}(t_0)} \left( \nu_i + \sum_{j:j \neq i} g_{ij}(t_0) p_j(t_0 + t^*) \right) .$$

Had the link gains been constant, the channel would have been supported from time  $(t_0 + t^*)$  and on. However, in a time varying case, the powers at time  $(t_0 + t^*)$  are appropriate only for the gain matrix at time  $t_0$ . To cope with this out-dated condition, we propose the following modification to the DCPC algorithm.

Accounting for the random link gains, the channel quality requirement has to be probabilistic. We require that for every time reference  $t_0$ , the conditional probability given the link gains and powers at time  $t_0$ , will satisfy

$$P_{t_0} (SIR_i(t_0 + t^*) \geq \gamma_i) \geq 1 - \beta . \quad (18)$$

Here,  $P_{t_0} (Y \in A) = P(Y \in A \mid \{g_{ij}(t_0)\}, \{p_i(t_0)\})$ , and  $\beta$  is a given positive parameter. Relaxing the standard notion in (2), we say that channel  $i$  is *supported at time  $t$*  if and only if (18) is satisfied. The selected parameter  $\beta$  is the outage probability.

Note that under the ideal convergence conditions above, if we could modify the DCPC algorithm in such a way that (18) would hold for every  $t_0$ , then the channel quality would have been satisfied for every time instant  $t > t^*$ . This objective is carried out in the remaining of this section, in which we specifically derive a scale up factor to the SIR target which is used in the DCPC.

First, we use the approximation in (11) to project appropriate percentiles for the link gains at time  $t_0 + t^*$ . In practice, the cochannel interference is dominated by a small number of interferers, to be denoted by  $N_0$  (usually 2 or 3). In this situation, even when the dominant interferers are unknown, we may still regard the interference as if it is being generated by  $N_0$  transmitters. Let  $0 < \beta_1 < 1$  and  $0 < \beta_2 < 1$ , be two parameters such that

$$\beta_2 (1 - \beta_1) = 1 - \beta , \quad (19)$$

where  $(1 - \beta)$  is the SIR quality parameter in (18).

We may now define the *Time Variant Power Control (TVPC)* with parameters  $(\beta_1, \beta_2, t^*)$ . Let  $\xi_1(t^*)$  be the  $1 - (1 - \beta_1)^{\frac{1}{N_0}}$  percentile of the normal random variable  $N(0, c^2 \cdot u \cdot t^*)$ , and  $(\xi_2(t^*) - 1)$  be its  $\beta_2$  percentile. That is,

$$P \left( N(0, c^2 u t^*) \geq \xi_1(t^*) \right) = 1 - (1 - \beta_1)^{\frac{1}{N_0}} , \quad (20)$$

and

$$P \left( N(0, c^2 u t^*) \geq \xi_2(t^*) - 1 \right) = \beta_2 . \quad (21)$$

### TVPC Algorithm

*For any given parameters  $(\beta_1, \beta_2, t^*)$ , every transmitter  $i$  updates its transmission power according to*

$$p_i(t+dt) = \begin{cases} \min \left\{ \bar{p}_i, \frac{\gamma_i}{\xi_2(t^*) \bar{g}_{ii}(t)} \left( \nu_i + (1 + \xi_1(t^*)) \sum_{j:j \neq i} \bar{g}_{ij}(t) p_j(t) \right) \right\} , & \text{if } i \in U(t), \\ p_i(t) , & \text{otherwise .} \end{cases} \quad (22)$$

**Remark 3.1** *In our numerical examples below we have used  $N_0 = 4$ . The difference however, in the scale up factor compared to the case with  $N_0 = 2$ , is at most 3%.*

Observe that under TVPC, powers are being updated as under DCPC but with a SIR target of  $\gamma_i (1 + \xi_1(t^*)) / \xi_2(t^*)$  rather than  $\gamma_i$ , and a background noise of  $\nu_i / (1 + \xi_1(t^*))$  rather than  $\nu_i$ . Also observe that TVPC is a power control algorithm that aims at maintaining the outage probability below a certain level  $\beta$ , whereas the DCPC algorithm aims at balancing the SIR values. Hence, TVPC is derived from a more practical objective function than DCPC is.

Thus, under the ideal conditions above, it follows from (15), (16) and (22), that

$$p_i(t_0 + t^*) = \min \left\{ \bar{p}_i, \frac{\gamma_i}{\xi_2(t^*) g_{ii}(t_0)} \left( \nu_i + (1 + \xi_1(t^*)) \sum_{j:j \neq i} g_{ij}(t_0) p_j(t_0 + t^*) \right) \right\}, \quad (1 \leq i \leq N), \quad (23)$$

for every realization of a gain matrix and power vector at time  $t_0$ .

Observe that the updated power for channel  $i$  is a function of the gains at time  $t_0$ . This is a result of averaging over many samples taken around time  $t$ , and our asymptotic properties in (16).

Let  $E_i$  be the event that for channel  $i$  the equality in (23) is attained by,

$$p_i(t_0 + t^*) = \frac{\gamma_i}{\xi_2(t^*) g_{ii}(t_0)} \left( \nu_i + (1 + \xi_1(t^*)) \sum_{j:j \neq i} g_{ij}(t_0) p_j(t_0 + t^*) \right).$$

Ignoring elements whose magnitude is the order of  $o(ut)^{1/2}$ , it follows from (11), (16), (19), (20) and (21) that follows )

$$\begin{aligned} P_{t_0} (SIR_i(t_0 + t^*) \geq \gamma_i \mid E_i) &\geq P_{t_0} (g_{ii}(t_0 + t^*) \geq \xi_2(t^*) g_{ii}(t_0)) \cdot \\ &\cdot P_{t_0} (g_{ij}(t_0 + t^*) \leq (1 + \xi_1(t^*)) g_{ij}(t_0) \mid \forall j \in N_0) \\ &= P ( N(0, c^2 u t^*) \geq \xi_2(t^*) - 1 ) \cdot [P ( N(0, c^2 u t^*) \leq \xi_1(t^*) )]^{N_0} \\ &= \beta_2 \cdot (1 - \beta_1) = 1 - \beta. \end{aligned} \quad (24)$$

This is the condition we were aiming at. Thus, under the TVPC algorithm every transmitter whose power converges to a value below the maximum transmission power, is supported. The reader should not confuse between the property given in (24) and the outage probability of channel  $i$ . The latter is upper bounded by  $P(\bar{E}_i)$ , and it depends on the cell plan, reuse factor and SIR target.

Note that the TVPC algorithm as defined in (22), requires the knowledge of both the interference power and the noise power, which may be difficult to measure in practice. A more practical version of the TVPC algorithm is the following one, which requires only the sum of the powers above. It is similarly formulated except for a noise scale up in (22), by a factor of  $(1 + \xi_1(t^*))$ . Let

$$\xi(t^*) = \frac{1 + \xi_1(t^*)}{\xi_2(t^*)}, \quad (25)$$

then every transmitter  $i$  updates its transmission power according to

$$p_i(t + dt) = \begin{cases} \min \left\{ \bar{p}_i, \frac{\gamma_i \xi(t^*)}{\bar{g}_{ii}(t)} \left( \nu_i + \sum_{j:j \neq i} \bar{g}_{ij}(t) p_j(t) \right) \right\}, & \text{if } i \in U(t), \\ p_i(t), & \text{otherwise.} \end{cases} \quad (26)$$

As above, for every channel  $i$  where

$$p_i(t_0 + t^*) = \frac{\gamma_i \xi(t^*)}{g_{ii}(t_0)} \left( \nu_i + \sum_{j:j \neq i} g_{ij}(t_0) p_j(t_0 + t^*) \right),$$

it is straightforward to show that

$$P_{t_0} (SIR_i(t_0 + t^*) \geq \gamma_i \mid E_i) \geq g_{ij}(t_0) \mid \beta_2 \cdot (1 - \beta_1) = 1 - \beta. \quad (27)$$

**Remark 3.2** *In an interference limited system, the noise power is much smaller than the cochannel interference power. Thus, one may expect only marginal differences in the transmission powers and the outage probabilities between the two versions of the TVPC algorithm. This is indeed supported by our numerical examples.*

As mentioned above, the conditional probabilities in (24) and (27) are **not** the outage probabilities. It is well recognized that analytical derivation of the system outage probability is intractable, and therefore we derive it by a simulation described in the next section.

Note that TVPC differs from DCPC by the scale up factor  $\xi(t^*)$  which has the following two degrees of freedom for the design. A fraction  $\beta$  that reflects the error correction capability, and an expected time horizon  $t^*$  for power stabilization. From Equation (24) one may observe that the scale up factor is determined by the following system parameters: the number of interferers  $N_0$ , the *normalized velocity*  $u$ , and the log variance of the shadow

fading  $\sigma^2$ . The actual number of interferers  $N_0$ , is not crucial in practice as pointed out in Remark 3.1. Thus, TVPC (compared with DCPC) requires only the mobile speed  $v$ , the effective correlation distance  $X$ , and the log variance of the shadow fading  $\sigma^2$ .

for TVPC. correlation distance of the shadow fading. How can these parameters be estimated in practice? The mobile speed can be taken as the maximum speed, a case that reflects a worst case scenario (see the results in Figure 8). One may also take the the actual instantaneous speed during the power control process, by applying good real-time speed estimators (see e.g. [7, 28]). The effective correlation distance and the log normal variance of the shadow fading can be taken from field measurements in the area where the cellular system is installed. Note that in general, urban environments have higher *normalized velocity* than rural environments, in spite of their higher vehicular speed.

Note that there are many combinations of  $\xi_1(t^*)$  and  $\xi_2(t^*)$  satisfying (19), and yielding the same value of  $\xi(t^*)$ . Furthermore, the feasible  $\xi(t^*)$  may range from a minimum value denoted by  $\xi_{min}(t^*)$ , to infinity. A question then rises, which one is best. Since a too high quality target may result in too high transmission powers, and consequently, too high interference powers and larger outage, one may argue for selecting the minimum required SIR target  $\xi_{min}(t^*)$ , which covers the individual channel variability. As we will see in the next section, this strategy is close to the optimal one.

To summarize, we may state that the essence of the TVPC algorithm is in its computation of the scale up factor required when mobility is taking into account. It can be referred to as the *transmission power cost of mobility*.

## 4 Numerical Results

In this section we evaluate the performance of the TVPC algorithm in a microcellular system. Although the vehicular speed is typically lower in this environment compared with a macrocellular (rural) environment, the normalized velocity in Equation (7) is higher due to a much smaller effective correlation distance. Since the scale up factor is monotonically increasing with the normalized velocity, we obtain higher scale up factors for microcellular environments. Hence, our numerical results present a worst case scenario for the proposed algorithm.

We compare its performance with that of DCPC, fixed transmission power (no power control), and constant received power control. The evaluation is made for several practical SIR target values.

## Manhattan-like microcellular environment

This is a typical metropolitan environment consisting of building blocks of a square shape. Streets are running between the building blocks in two directions, horizontal and vertical. In our simulation we assume that each block is of length 100 *m*. We further assume that radio-waves can propagate only along the streets.

We study the power control algorithms for two different cell plans. The first one is an Asymmetric Half Square (AHS) cell plan, depicted in Figure 1. The cluster size  $N_c = 3$ , and the *line-of-sight* (*LOS*) reuse distance is  $D_{LOS} = 3$ . This cell plan is denoted by AHS(1,1,3), in agreement with the notation in [16]. (The notation from there is extended to include also the cluster size.)

The second cell plan (Figure 2) which we consider is an Asymmetric Half Square cell plan with cluster size  $N_c = 4$ . The corresponding LOS reuse distance is  $D_{LOS} = 4$ , and the cell plan is denoted by AHS(1,1,4). From our numerical results it appears that the outage probability curve as a function of the SIR target in AHS(1,1,4), is a shift of the curve obtained for AHS(1,1,3). This is explained by the fact that the distance between two LOS interferers is also a shift of each other. Therefore, most of our results are presented only for the AHS(1,1,3) case.

In both cell plans, one base station is placed in every street corner at lamp-post level. Base stations use omnidirectional antennas and the cell size is assumed to be half a block in all four directions. In the simulation, we take 48 cochannel cells for AHS(1,1,3), and 64 cochannel cells for AHS(1,1,4). For each cell plan we use a fixed channel assignment scheme which divides the cells into  $N_c$  different channel groups.

To model the large scale propagation loss, set  $(x_i, y_i)$  and  $(x_j, y_j)$  to be mobile  $i$  and base station  $j$  coordinates, respectively. Denote by  $x = |x_i - x_j|$  and  $y = |y_i - y_j|$ , the horizontal and the vertical distances, respectively, between the mobile and the base station. From [10],

the large scale propagation loss between mobile  $i$  and base station  $j$  can be modeled by

$$L_{ij} = \left[ 16 \frac{\pi^2 f^2}{c^2} \left( xye^{-\left(\frac{20W_x W_y}{xy}\right)} + x + y + 10 \right)^2 \left( 1 + \sqrt{\left(\frac{x+y}{L_n}\right)^{(2n-4)} + \left(\frac{x^2+y^2}{L_m^2}\right)^{(m-2)}} \right) \right]^{-1},$$

where  $c$  is the speed of light,  $f$  is the transmission frequency, and  $W_x$  and  $W_y$  are the street widths in the horizontal and vertical direction, respectively. The parameters  $n$ ,  $L_n$ ,  $m$  and  $L_m$  are all propagation constants, [10]. In our simulation we use  $f = 900 \text{ MHz}$ ,  $W_x = W_y = 25 \text{ m}$ ,  $n = 4$ ,  $m = 25$ ,  $L_n = 200 \text{ m}$  and  $L_m = 700 \text{ m}$ . From the measurement data in [17], we take the standard deviation of the shadow fading to be  $\sigma = 4 \text{ dB}$  and the correlation distance  $X = 8.3 \text{ m}$ .

The median *Signal to Noise Ratio (SNR)* at a cell border under the maximum transmission power is calibrated to  $82 \text{ dB}$ . That is, we take a strongly interference limited system.

The starting position of the new mobiles are independently sampled from a uniform distribution over each cell area, and their travel directions (right, left, up or down) are chosen with equal probabilities. Moreover, mobiles move along the streets with a constant speed of  $30 \text{ km/h}$ . At street corners, they turn left or right, or continue straight ahead with equal probabilities.

We further assume that call durations are independent and geometrically distributed with a mean of  $120 \text{ seconds}$ .

## Method of comparison

The prime criterion by which we compare the algorithms is the *outage probability* evaluated by the following simulation. We maintain a fixed number of mobiles in the system by replacing every mobile which exits a cell, with a new one in a random location. A mobile disconnection and a mobile transition to another cell, are both regarded as mobile exits. The system is initialized with all mobiles transmitting according to the fixed-point power vector solution in (14), with respect to the instantaneous gain matrix. For every power control algorithm and SIR target, we simulate 10,000 calls (i.e., mobile exits).

For each mobile, we accumulate the proportion of time where  $SIR_i(t) \geq \gamma_i$ . If this proportion is greater than  $1 - \beta$ , then the mobile is supported, otherwise it is not supported.

In the simulations, we take  $\beta = 0.05$ . The outage probability under a given power control algorithm is estimated by the proportion of unsupported mobiles.

**Note that although TVPC is designed to achieve an outage probability below  $\beta$ , it may not be attainable for any load. What TVPC actually does achieve is the following. For those mobile whose short term average  $SIR(t)$  equals the scaled up SIR target, the probability of dropping below the non scaled up SIR target is less than  $\beta$ . At high loads, there will be mobiles for which their short term average  $SIR(t)$  cannot be equal to the scaled up SIR target. Those mobiles also contribute to the outage probability, which may therefore exceed  $\beta$ .**

We confine our examples to the uplink case and synchronous power updates. The time between two power updates is denoted by  $\Delta t$ . We further assume a constant SIR target,  $\gamma_i = \gamma^t$ , for all mobiles. We compare the TVPC outage probability with that of a fixed transmission power (all transmitters use the maximum transmitter power), constant-received power control, and DCPC. Under the constant-received power control, the transmitters update their power according to,

$$p_i(t + \Delta t) = \frac{C}{\bar{g}_{ii}(t)},$$

where the target power  $C$  is determined by a desired SNR of 63 dB, when the transmission power is less than the maximum value.

Most notable is the fact that the classical DCPC algorithm has an extremely high outage probability. To shade some light on this result we also evaluate the ratio

$$\Delta I = \left( \frac{\nu_i + \sum_{j:j \neq i} g_{ij}(t + dt) p_j(t + dt)}{g_{ii}(t + dt)} \right) / \left( \frac{\nu_i + \sum_{j:j \neq i} \bar{g}_{ij}(t) p_j(t)}{\bar{g}_{ii}(t)} \right).$$

This is the ratio between the desired updated power, and the actually updated power. Its symmetric distribution depicted below, explains the high outage probability under DCPC.

We investigate the performance of the TVPC algorithm with different scale up factors. As will be seen in the figures below, the outage probability decreases when the scale up factor increases until a certain threshold. From there on the outage probability starts to increase (due to too much interference in the network caused by a too high scale up factor). Naturally, the optimal selection of the scale up factor is the one for which the minimum



outage probability is attained. Finding it is mathematically intractable, however in the simulation we can use a binary numerical search to find it.

## Results

Figure 3 depicts the outage probability in the AHS(1,1,3) cell plan, under TVPC with different scale up factors  $\xi$  values (2, 2.5, 3, 4 dB). The minimum value of  $\xi$  according to (19) and (25) is  $\xi_{min} = 2.5$  dB. The time horizon is taken to be  $t^* = 10$  ms, which equals  $\Delta t$  (i.e., one update within  $t^*$ ).

Observe that the outage probability significantly decreases as the factor  $\xi$  decreases to  $\xi_{min}$ . The lowest outage probability is obtained by a factor slightly higher than  $\xi_{min}$  (for  $\xi = 3$  dB). A further increase in  $\xi$  results in an increase in the outage probability. Thus, the TVPC predicted scale up factor is very close to the optimal one.

The classical DCPC algorithm corresponds to a TVPC with  $\xi = 1$  (0 dB). From our simulations *it turns out that the DCPC algorithm which updates the powers according to (12), yields an outage probability close to one (independently of the SIR target)*. This result is explained by the almost symmetric distribution of  $\Delta I$  around 1 (0 dB), which is depicted in Figure 4. The probability that  $\Delta I$  will be greater than 1 (0 dB) is 56%. That is, with a probability of 0.56, the updated power under DCPC is lower than the required power. With such an instantaneous under-power update, a mobile could not maintain a proper SIR level for 95% of its time. That is, it will most likely experience an outage. This behavior of the classical DCPC algorithm demonstrates why the SIR target needs a scale up. According to Figure 3, the TVPC predicted factor results in outage probabilities which are quite close to the optimal ones.

The extremely high outage under DCPC can be reduced by using a minimum transmitter power level in the algorithm. The performance curves under the DCPC algorithm in the subsequent figures, uses a DCPC with a dynamic range of 60 dB. We note that the TVPC algorithm successfully copes with the mobility of the users and does not experience the same problem as DCPC does. We also examined the effect of a minimum transmitter power in the TVPC algorithm (a 60 dB dynamic range as in DCPC). It appears that the outage probability can be reduced for some SIR targets under which most mobiles can be supported. The improvement however, is marginal and for higher or lower outage levels, there is none.

To examine how the time horizon  $t^*$  affects the TVPC algorithm, we depict in Figure 5 a graph corresponding to Figure 3, but with a time horizon of  $t^* = 100 \text{ ms}$ . As in Figure 3, the time between two power updates is taken to be  $\Delta t = t^*$ , (i.e., one power update within  $t^*$ ). The minimum scale up factor  $\xi$  in this case is  $\xi_{min} = 8.55 \text{ dB}$ . Observe that here, the outage probability can be improved if we use a factor smaller than  $\xi_{min}$ . The lowest outage probability is obtained for  $\xi = 7 \text{ dB}$ . Again, as we increase the scale up factor  $\xi$ , the outage probability increases. As in the case with  $t^* = 10 \text{ ms}$ , the TVPC predicted scale up factor results in outage probabilities which are quite close to the optimal ones.

In Figure 6, we illustrate the TVPC performance as function of the time horizon  $t^*$ . (Figures 3 and 5 are presented using the same scale). Note that there is a trade-off between the outage probability and the power update rate. To compensate a slow power update rate, one must use a higher scale up factor  $\xi$ . This evidently results in a lower radio spectrum utilization.

Another interesting question is how the number of power updates within a single time horizon  $t^*$  affects the performance. In Figure 7, we show the performance for different values of  $\Delta t$  (100, 50, 10  $\text{ms}$ ), when  $t^* = 100 \text{ ms}$ , and the minimum factor of  $\xi_{min} = 8.55 \text{ dB}$ . We have found that the difference in the outage probabilities is less than 1% for any SIR target. Similar results have been obtained for  $t^* = 10 \text{ ms}$ , when using the minimum factor  $\xi_{min} = 2.5 \text{ dB}$ . Thus, the number of power updates within  $t^*$  appears to have a negligible affect.

The selection of  $\xi$  depends on the mobile speed  $v$ , and the correlation distance  $X$ . A higher normalized speed  $u$ , results in a larger fading variation, and consequently in a higher factor  $\xi$ . The velocity  $v$  can be interpreted as a system parameter corresponding to the “fastest” moving class of users. That is, if we design the system to handle this class of users, it should also be able to support a mixture of users moving at different speeds. To test this design assumption, we compare in Figure 8, the performance of the TVPC algorithm for two different cases. One where all users move at speed 30  $\text{km/h}$ , and the other where users speed are sampled from a uniform distribution in the interval  $[0, 30] \text{ km/h}$ . As expected, the outage probability is lower for the case where the speeds may vary.

Finally, in Figures 9, 10 and 11, we compare the performance of the TVPC algorithm using  $\xi_{min}$ , with the performance under *Fixed Transmission Power (Fixed Tx-power)*, *DCPC*

(using a minimum transmitter power level) and *Constant received* power control. Figure 9 presents the outage probabilities in the AHS(1,1,3) cell plan with  $t^* = 10 \text{ ms}$ , Figure 10 in the AHS(1,1,3) cell plan with  $t^* = 100 \text{ ms}$ , and Figure 11 in the AHS(1,1,4) cell plan with  $t^* = 10 \text{ ms}$ .

Observe that the TVPC algorithm is significantly better than any other power control algorithm. At the 10% outage probability level, a SIR gain of about 6 dB can be achieved compared to a fixed transmission power scheme, and about 4.5 dB compared to a constant received power control algorithm, when considering the AHS(1,1,3) cell plan with  $t^* = 10 \text{ ms}$ . The corresponding gains in the AHS(1,1,3) cell plan with  $t^* = 100 \text{ ms}$ , are 3.5 dB and 3 dB, respectively. In the AHS(1,1,4) cell plan with  $t^* = 10 \text{ ms}$ , the SIR gains are 5 dB and 4 dB, respectively. At the 5% outage probability level, a SIR gain of about 6.5 dB can be achieved compared to a fixed transmission power scheme, and about 4.5 dB compared to a constant received power control algorithm, when considering the AHS(1,1,3) cell plan with  $t^* = 10 \text{ ms}$ . The corresponding gains in the AHS(1,1,3) cell plan with  $t^* = 100 \text{ ms}$ , are 4.5 dB and 3.5 dB, respectively. In the AHS(1,1,4) cell plan with  $t^* = 10 \text{ ms}$ , the SIR gains are 5.5 dB and 4 dB, respectively. Similar improvements are also obtained for lower outage probabilities. Thus, in spite of the scale up factor that we apply in the TVPC algorithm compared to the DCPC algorithm, a substantial improvement in capacity is obtained.

It is interesting to relate the performance of the TVPC algorithm to the performance of the power control algorithm in the IS-95 CDMA system which uses 800 power updates per second. For the latter, a scale up factor around 3 dB is required for high speed mobiles. From the numerical results for the TVPC algorithm, we find that at a rate of 100 power updates per second in an urban environment, only a scale up factor of 2.5 dB is required. Clearly, if TVPC would use 800 power updates per second, the scale up factor would be significantly smaller. Moreover, as noted above, microcellular environments are less favorable than macrocellular environments.

## 5 Conclusions

We close with the following main conclusions.

In practice link gains are time varying, and the classical DCPC algorithm has an outage probability close to one, unless some counter-measures are taken. One is to bound the

transmitter power from below. The other is to scale up the SIR target. In the latter case, it is not clear however, with how much one needs to scale up the SIR target. The TVPC algorithm copes with this situation and provides a close to an optimal scale up factor.

Numerical results show that the TVPC algorithm provides a substantial decrease in outage probability on compared to the following algorithms: DCPC with a lower bound on the transmission power, constant-transmitted power, and constant-received power control. This indicates that a significant improvement in spectrum utilization can be obtained when using the TVPC algorithm.

## References

- [1] J. M. Aein. Power Balancing in Systems Employing Frequency Reuse. *Comsat Tech. Rev.*, Vol. 3, No. 2, 1973.
- [2] M. Almgren, H. Andersson and K. Wallstedt. Power Control in a Cellular System. Proc. IEEE Veh. Tech. Conf., VTC-94:833–837, 1994.
- [3] M. Andersin, Z. Rosberg and J. Zander. Gradual Removals in Cellular PCS with Constrained Power Control and Noise. *IEEE/ACM Wireless Networks*, Vol. 2, pp. 27–43, 1996. Radio Commun.
- [4] M. Andersin, Z. Rosberg and J. Zander. Distributed Discrete Power Control in Cellular PCS. *Wireless Personal Communications*, Vol. 6, No. 3, 1998. Multiaccess, Mobility and Teletraffic for Radio Commun. Personal
- [5] M. Andersin, Z. Rosberg and J. Zander. Soft Admission in Cellular PCS with Constrained Power Control and Noise. *IEEE/ACM Trans. on Networking*, Vol. 5, No. 2, 1997.
- [6] M. Andersin, M. Frodigh and K-E. Sunell. Distributed Radio Resource Allocation in Highway Microcellular Systems. Proc. 5th Winlab Workshop, Apr. 1995.
- [7] M. D. Austin and G. L. Stüber. Velocity Adaptive Handoff Algorithms for Microcellular Systems. *IEEE Trans. on Veh. Tech.*, Vol. 43, No. 3, Aug. 1994.
- [8] N. Bambos and G. J. Pottie. On Power Control in High Capacity Cellular Radio Networks. Proc. 3rd WINLAB Workshop, Oct., 1992.
- [9] N. Bambos, S. C. Chen and G. J. Pottie. Channel Access Algorithms with Active Link Protection for Wireless Communication Networks with Power Control. Technical Report, UCLA-ENG-95-114, Department of Electrical Engineering, UCLA, 1995.
- [10] J-E. Berg. A Simplified Street Width Dependent Microcell Path Loss Model. COST 231, TD(94)035, 1994.
- [11] J. A. Bucklew. *Large Deviation Techniques in Decision, Simulation, and Estimation*. J. Wiley and Sons, Inc., NY 1990.
- [12] G. J. Foschini. A Simple Distributed Autonomous Power Control Algorithm and its Convergence. *IEEE Trans. on Veh. Tech.*, Vol. 42, No. 4, 1993.
- [13] S. A. Grandhi, R. Vijayan and D. J. Goodman. A Distributed Algorithm for Power Control in Cellular Radio Systems. *IEEE Trans. on Veh. Tech.*, Vol. 42, No. 4, Nov. 1993. Computing,
- [14] S. A. Grandhi, R. Vijayan, D. J. Goodman and J. Zander. Centralized Power Control in Cellular Radio Systems. *IEEE Trans. on Veh. Tech.*, Vol. 42, No. 4, 1993.

- [15] S. A. Grandhi, J. Zander and R. Yates. Constrained Power Control. *Wireless Personal Communications*, Vol. 1, No. 4, 1995.
- [16] M. Gudmundson. Cell Planning in Manhattan Environments. Proc. IEEE Veh. Tech. Conf., VTC-92:435–438, 1992.
- [17] M. Gudmundson. Correlated Model for Shadow Fading in Mobile Radio Systems. *Electronics Letters*, Vol.27, No. 23, 2145–2146, 1991.
- [18] S. V. Hanly. Information Capacity of Radio Networks. Ph.D. Thesis, Cambridge University, Aug. 1993.
- [19] S. V. Hanly. An Algorithm for Combined Cell-site Selection and Power Control to Maximize Cellular Spread Spectrum Capacity. *IEEE JSAC, special issue on fundamentals of networking*, Vol. 13, No. 7, Sept. 1995. fundamentals
- [20] P. S. Kumar, R. D. Yates and J. Holtzman. Power Control with Bit Error Rates. Proc. MILCOM'95, San Diego, 1995. 1995.
- [21] J. C. Lin, T. H. Lee and Y. T. Su. Power Control Algorithm for Cellular Radio Systems. *IEEE Trans. on Veh. Tech.*, Vol.44, No. 1, Feb. 1995.
- [22] H. J. Meyerhoff. Methods for Computing the Optimum Power Balance in Multibeam Satellite. *Comsat Tech. Rev.*, Vol. 4, No. 1, 1974.
- [23] D. Mitra. An Asynchronous Distributed Algorithm for Power Control in Cellular Radio Systems. Proc. 4th WINLAB Workshop, Oct. 19-20, 1993.
- [24] D. Mitra and J. A. Morrison. A Distributed Power Control Algorithm for Bursty Transmissions on Cellular, Spread Spectrum Wireless Networks. Proc. 5th WINLAB Workshop, Apr. 1995.
- [25] R. W. Nettleton and H. Alavi. Power Control for Spread-spectrum Cellular Mobile Radio System. Proc. IEEE Veh. Tech. Conf., VTC-83:242–246, 1983.
- [26] Z. Rosberg. Fast Power Control in Cellular Networks Based on Short-Term Correlation of Rayleigh Fading. Proc. 6th WINLAB Workshop, Apr. 1997.
- [27] Z. Rosberg and J. Zander. Power Control in Wireless Networks with Random Interferers. TRITA-XX 95-xx, ISSN xxxx-xxxX, ISRN KTH/xx/R-95/xx-SE, Radio Commun. Systems., KTH, Sweden, Dec. 1995.
- [28] A. Sampath and J. M. Holtzman. Estimation of Maximum Doppler Frequency for Handoff Decisions. Proc. IEEE Veh. Tech. Conf., VTC-93:859–862, 1993.
- [29] R. Yates and C. Y. Huang. Integrated Power Control and Base Station Assignment. *IEEE Trans. on Veh. Tech.*, Vol. 44, No. 3, Aug. 1995.
- [30] R. Yates. A Framework for Uplink Power Control in Cellular Radio Systems. *IEEE JSAC*, Vol. 13, No. 7, Sept. 1995.

- [31] J. Zander. Transmitter Power Control for Co-channel Interference Management in Cellular Radio Systems. Proc. 4th WINLAB Workshop, Oct. 19-20, 1993.
- [32] J. Zander. Performance of Optimum Transmitter Power Control in Cellular Radio Systems. *IEEE Trans. on Veh. Tech.*, Vol. 41, No. 1, 1992.
- [33] J. Zander. Distributed Cochannel Interference Control in Cellular Radio Systems. *IEEE Trans. on Veh. Tech.*, Vol. 41, No. 3, 1992.

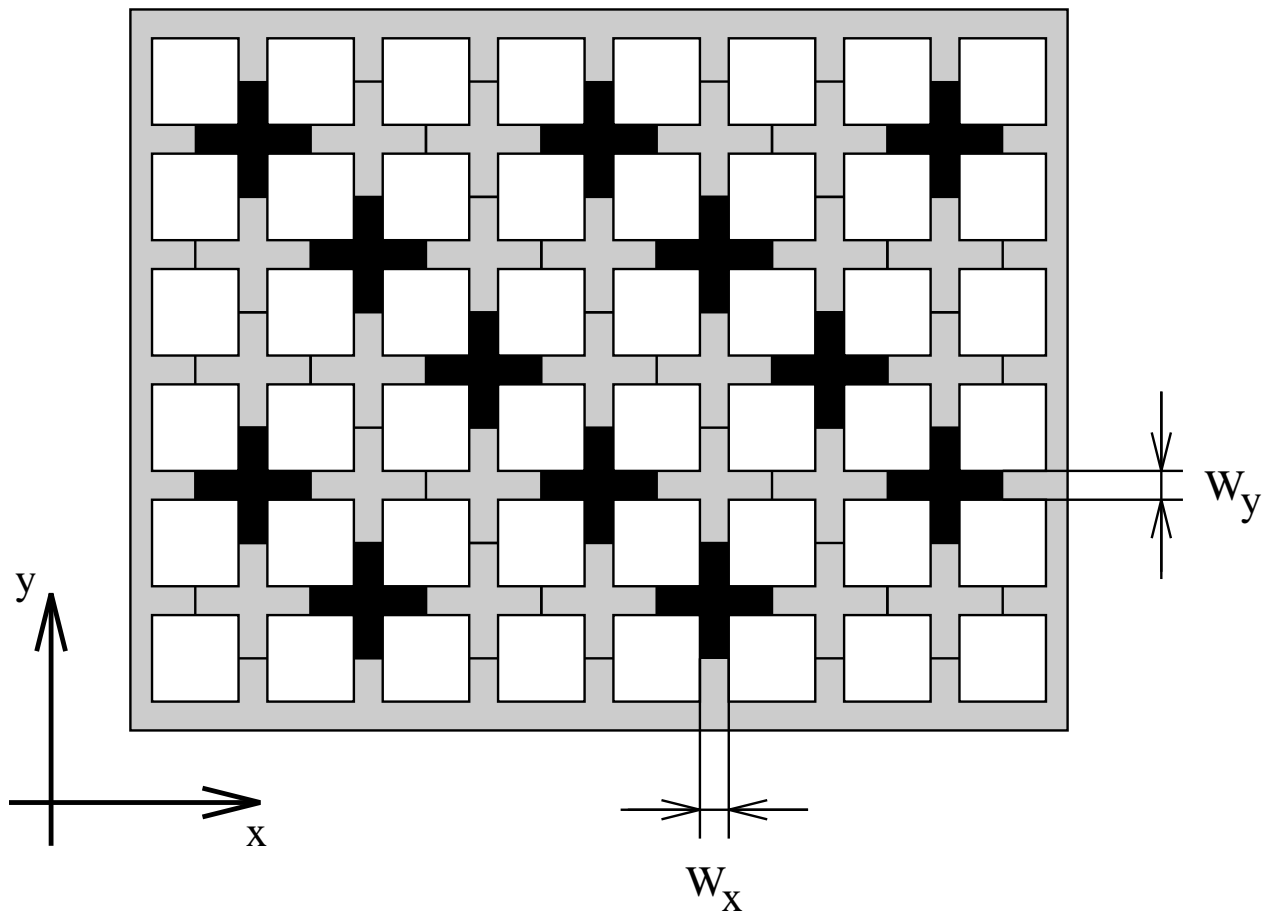


Figure 1: The asymmetric AHS(1,1,3) cell plan with cluster size  $N_c = 3$ . The dark crosses are the cochannel cells and the white squares are the buildings seen from above.



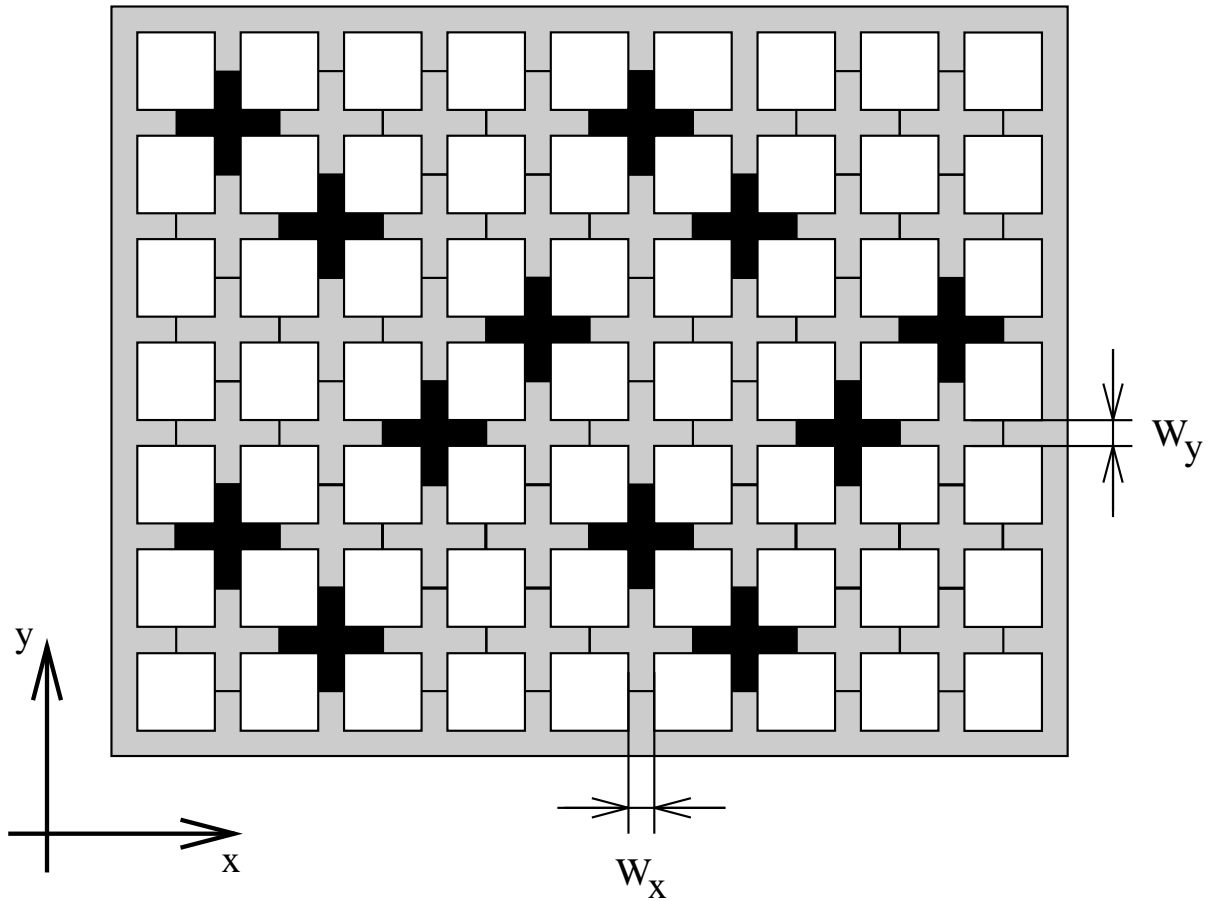


Figure 2: The asymmetric AHS(1,1,4) cell plan with cluster size  $N_c = 4$ . The dark crosses are the cochannel cells and the white squares are the buildings seen from above.

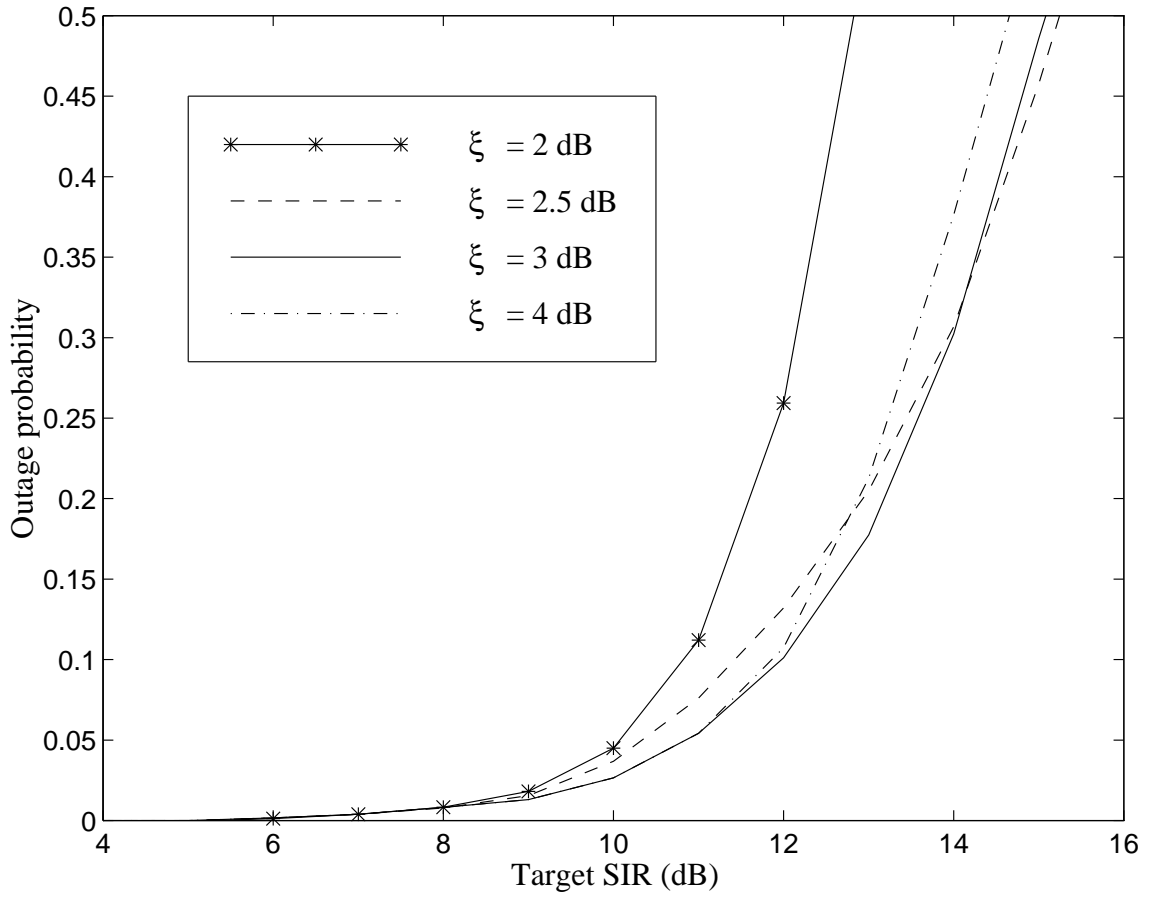


Figure 3: The outage probability under TVPC as a function of the SIR target and different values of the boosting factor  $\xi$ , in AHS(1,1,3) with 48 cochannel cells and  $t^* = 10$  ms. The minimum value of  $\xi$  is 2.5 dB.

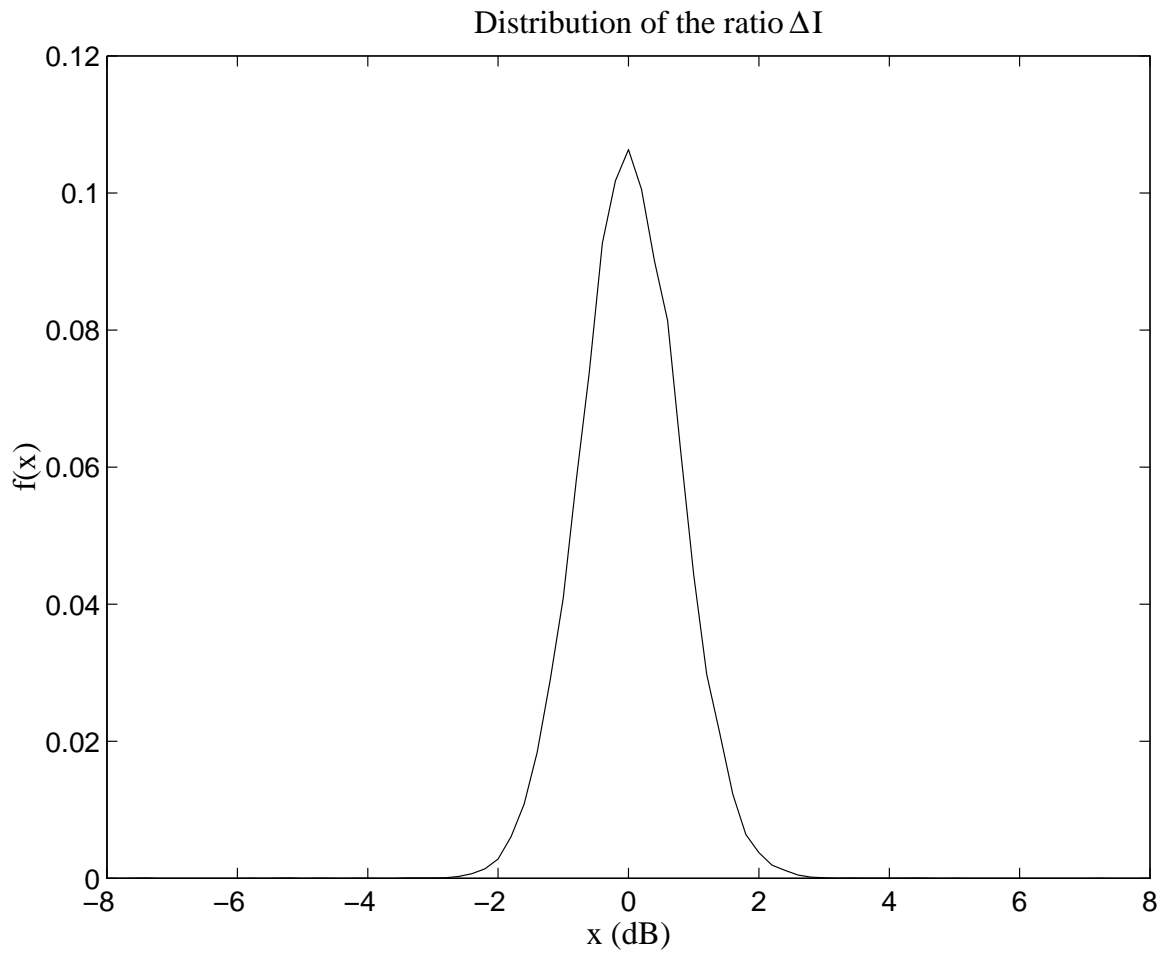


Figure 4: The distribution of the ratio  $\Delta I$  when the DCPC algorithm is used with  $\Delta t = 10 \text{ ms}$  and at a SIR target of  $9 \text{ dB}$ .

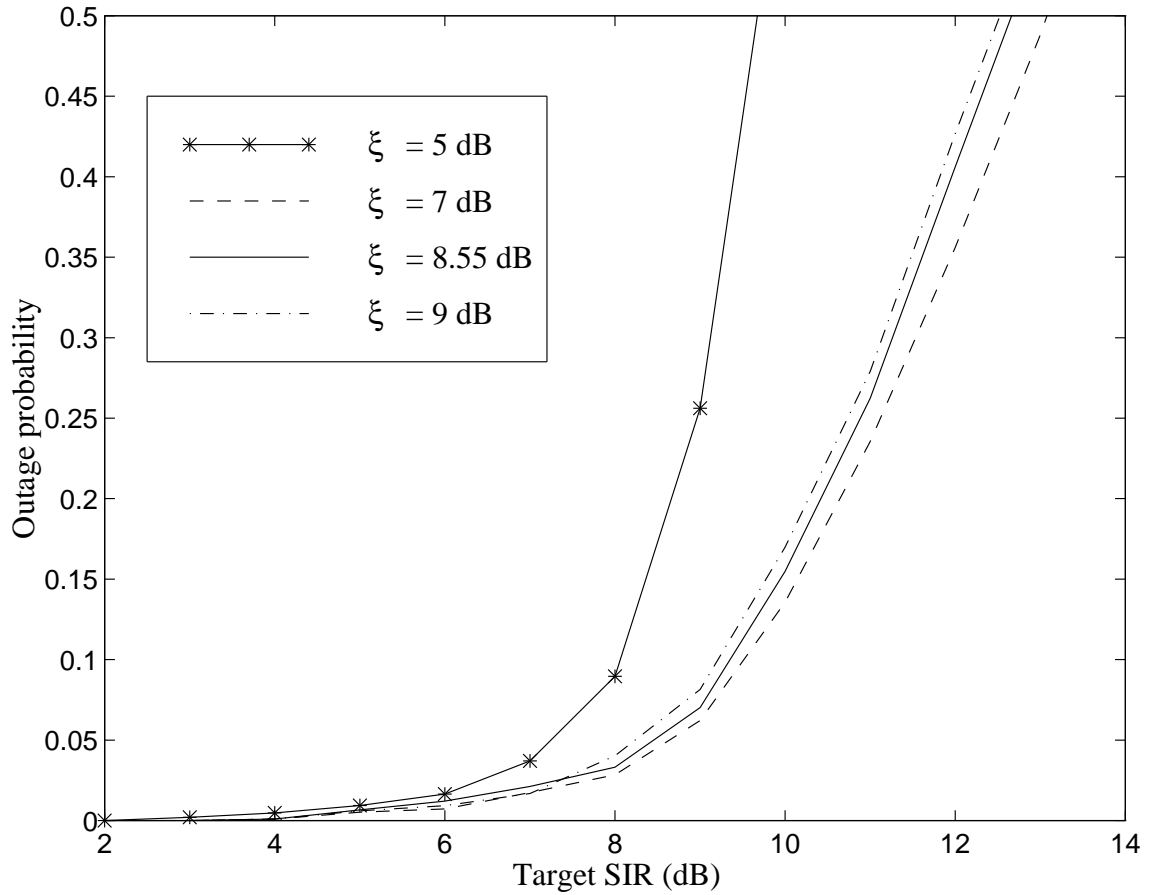


Figure 5: The outage probability under TVPC as a function of the SIR target and different values of the boosting factor  $\xi$ , in AHS(1,1,3) with 48 cochannel cells and  $t^* = 100$  ms. The minimum value of  $\xi$  is 8.55 dB.

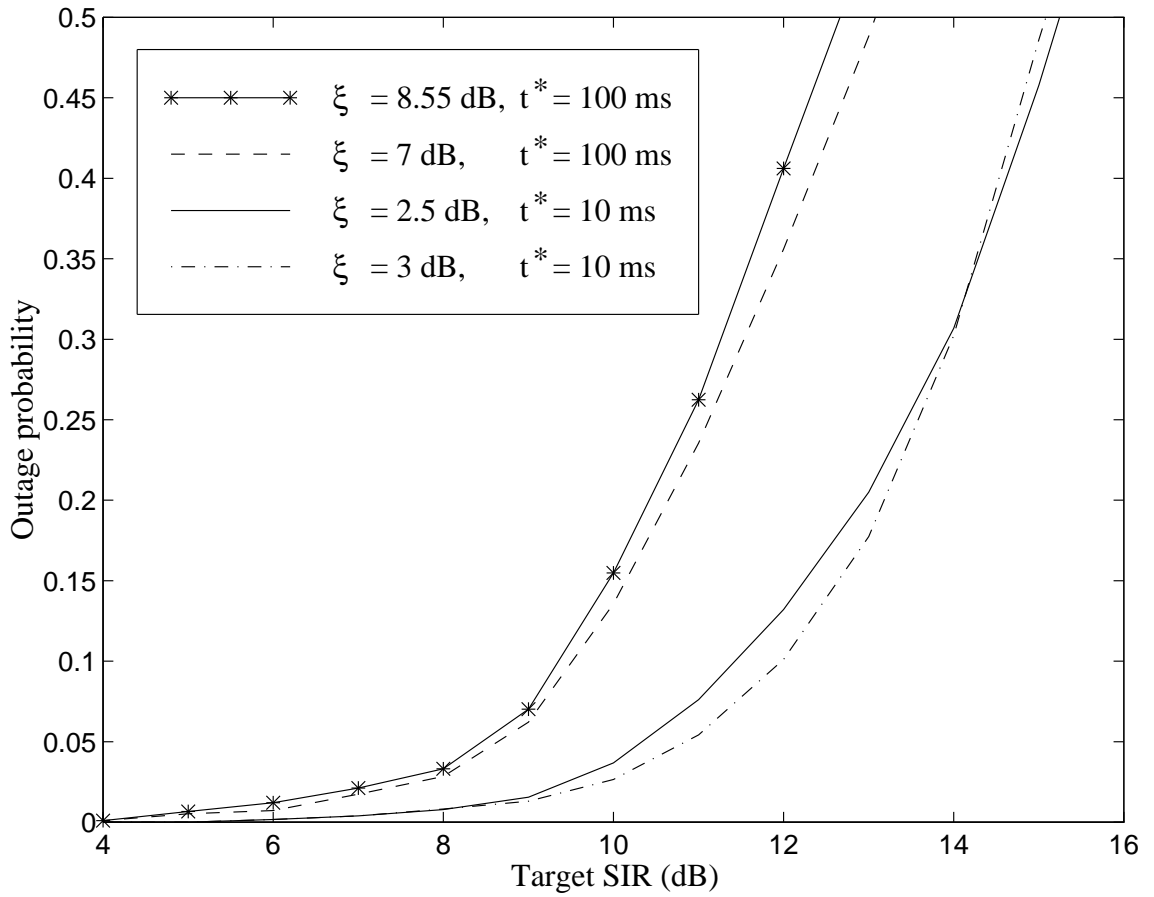


Figure 6: The outage probability under TVPC as a function of the SIR target and different values of time horizons  $t^*$ , in AHS(1,1,3) with 48 cochannel cells.

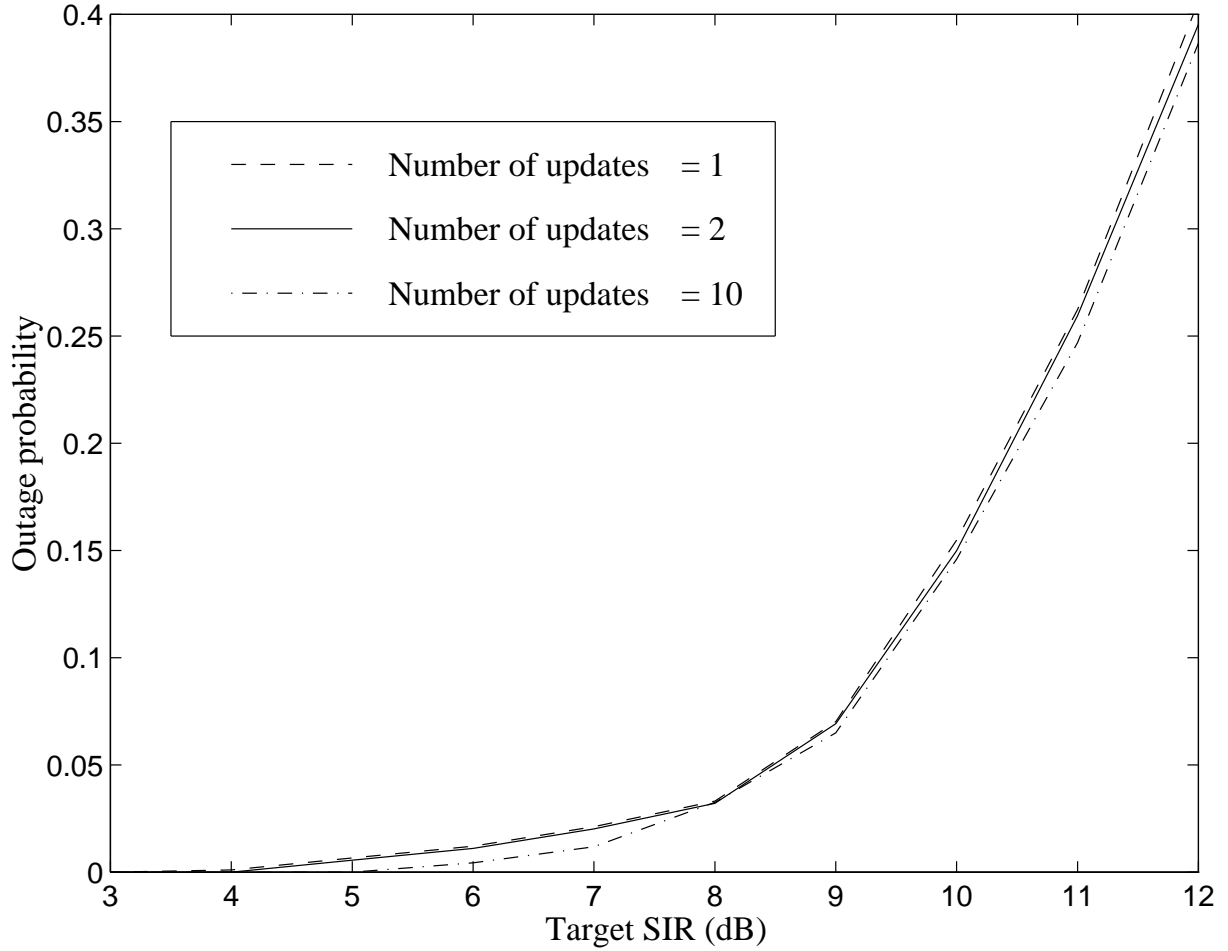


Figure 7: The outage probability under TVPC as a function of the SIR target and different number of power updates within the time horizon  $t^* = 100 \text{ ms}$ , in AHS(1,1,3) with 48 cochannel cells. The number of updates 1,2,10 correspond to  $\Delta t = 100, 50, 10 \text{ ms}$ . The value of  $\xi = 8.55 \text{ dB}$ .

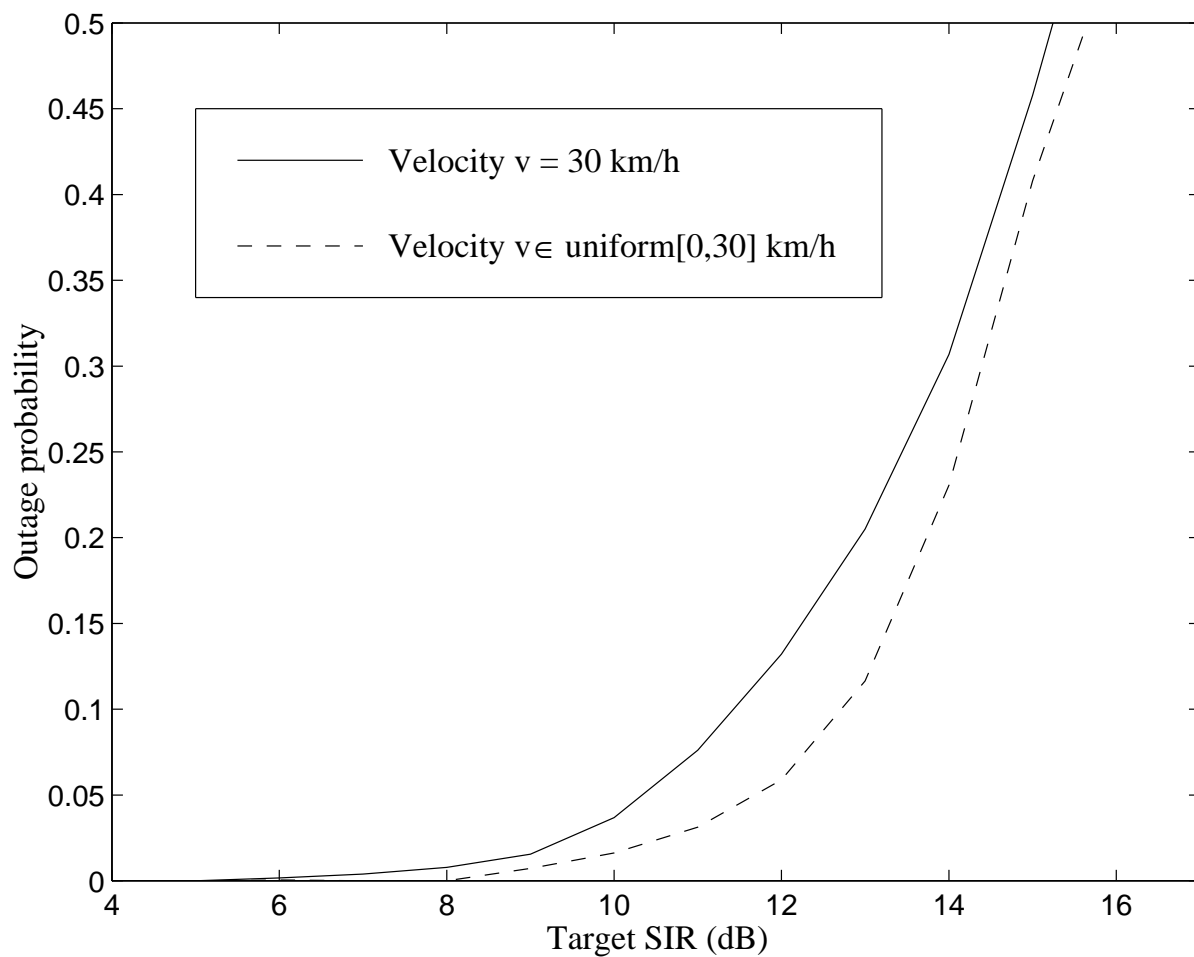


Figure 8: The outage probability under TVPC as a function of the SIR target and different types of traffic in AHS(1,1,3) with 48 cochannel cells. The factor  $\xi = 2.5 \text{ dB}$  and the time between two power updates  $\Delta t = 10 \text{ ms}$ .

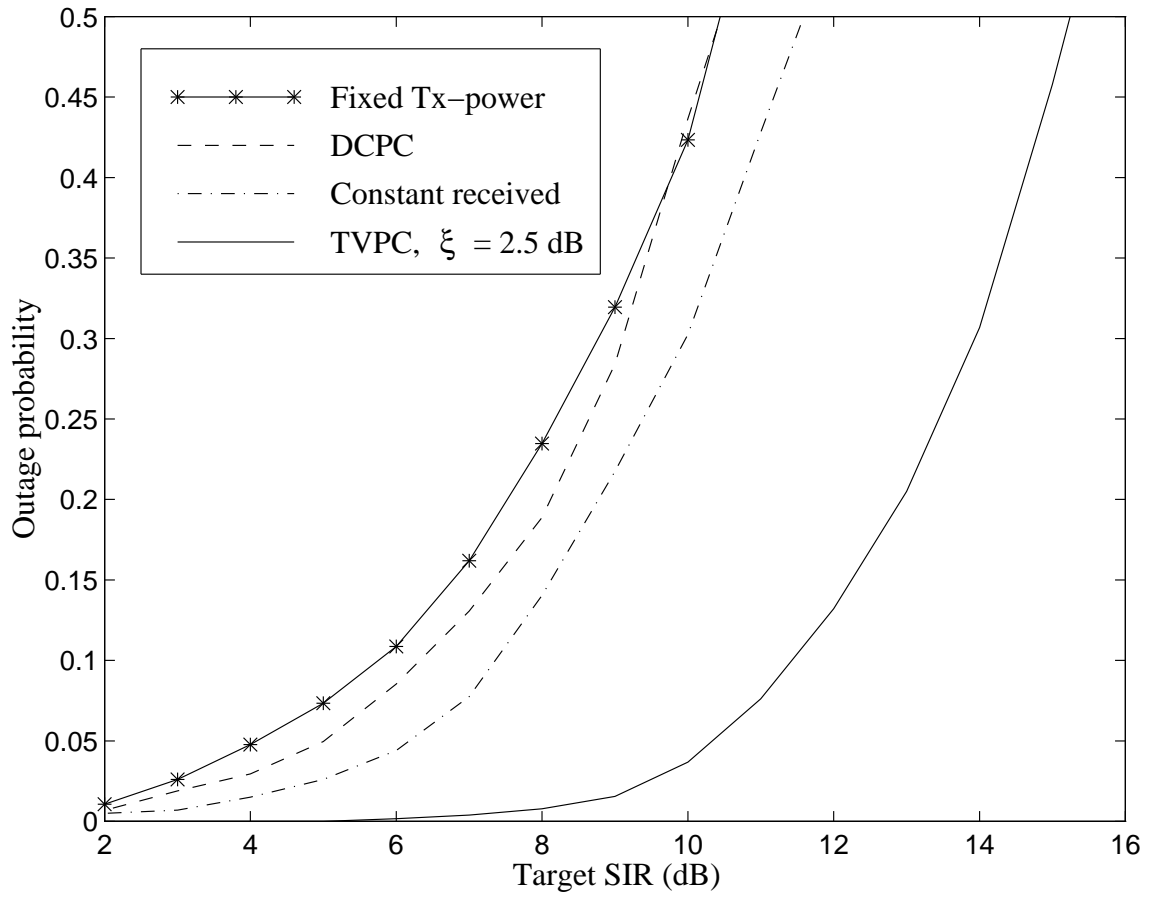


Figure 9: Outage probability comparison in the AHS(1,1,3) cell plan with 48 cochannel cells, when  $\Delta t = t^* = 10$  ms.



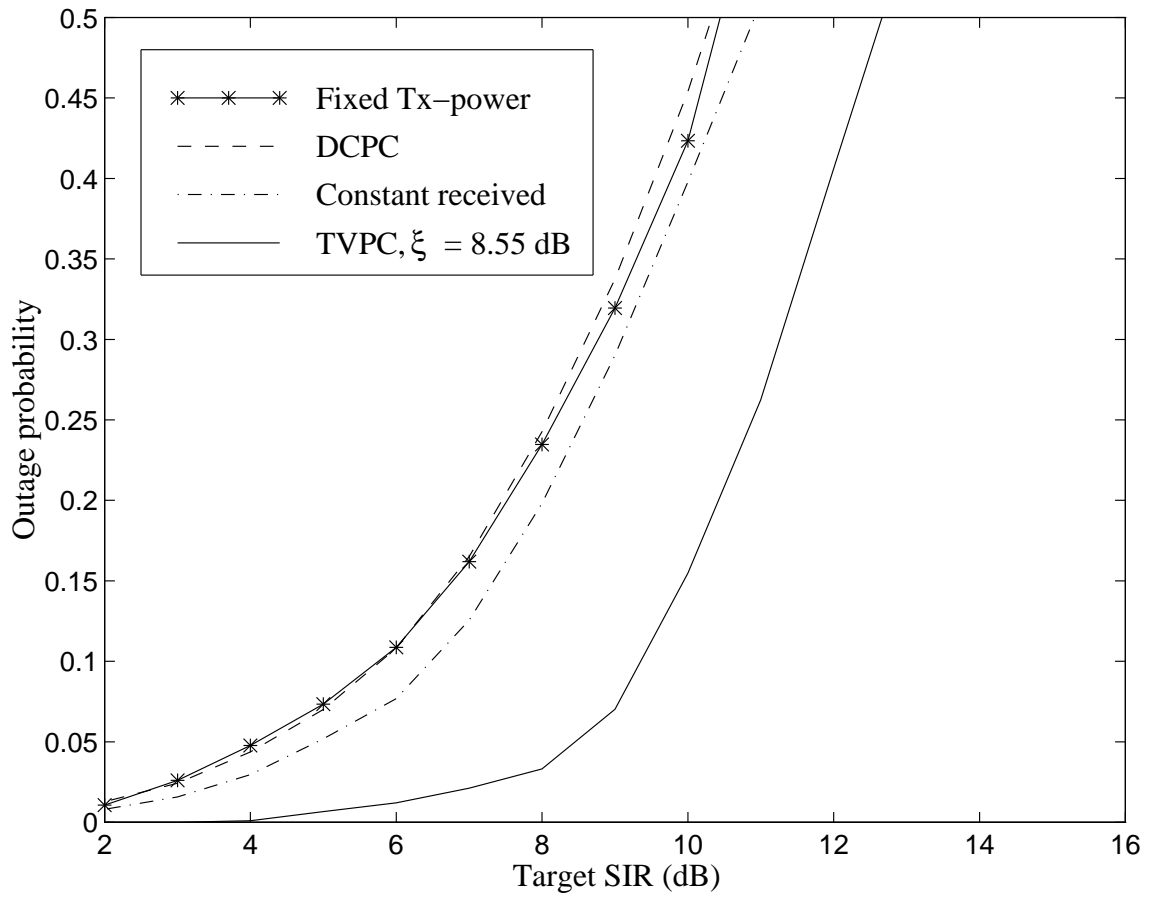


Figure 10: Outage probability comparison in the AHS(1,1,3) cell plan with 48 cochannel cells, when  $\Delta t = t^* = 100$  ms.

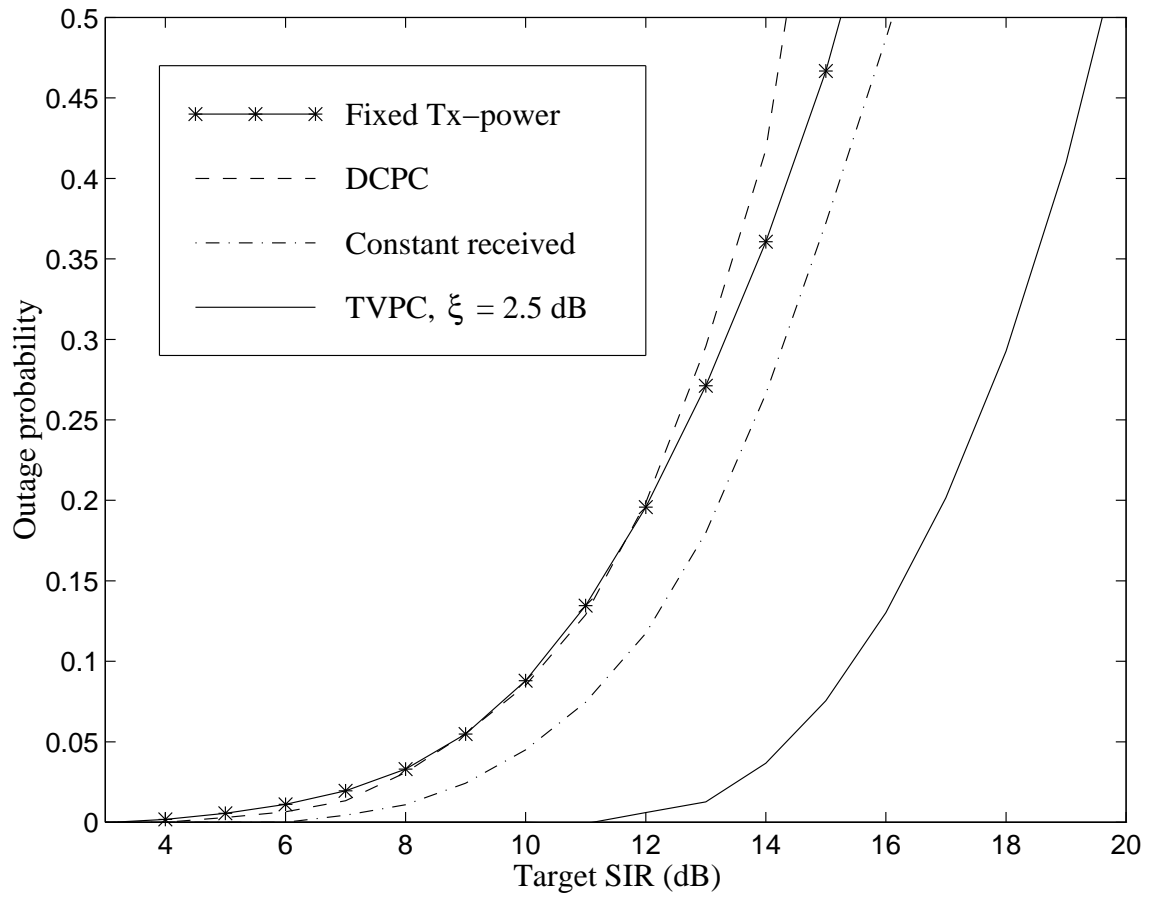


Figure 11: Outage probability comparison in the AHS(1,1,4) cell plan with 64 cochannel cells, when  $\Delta t = t^* = 10$  ms.